4

Solar Convective Furnace

4.1. INTRODUCTION

Some of the metal processing operations, such as heat treatment, require a furnace that can operate at a temperature below 1000 °C. The heat sources in these furnaces are either electricity, produced from the conventional power plant, which is produced by using fossil fuel or by direct heating by burning fuel. Both lead to the production of greenhouse gasses such as CH_4, CO_2, N_2O, etc. resulting in global warming [Latake 2015]. Consequently, the metals processing operations provide tremendous opportunities for the use of concentrated solar power as a high-temperature heat source. Hence solar energy can be used as a green option for process heating, metal processing, sintering, foaming, joining, coating, syngas production, etc. [Elington *et al.* 2013] [Herranz *et al.* 2010] [Villafán-Vidales *et al.* 2017] [Fernández-González *et al.* 2018].

Solar energy has been used from years. It is believed that use of solar energy is made in purpose from 7th century B.C. In early 212 B.C. Greek scientist Archimedes, used bronze shields to focus sunlight to set fire in wooden ships of Roman. In 1772, Lavoisier built a large magnifying glass to focus sunlight for combustion of metal in a glass sealed container which achieved 1773 °C. In 1921, a paraboloidal concentrator type solar furnace is built by Straubel in Germany that could reach temperature in the vicinity of 3000^{0}C [Duwez *et al.* 1956]. Further many developments in use of this energy occur and it is still going on. A Solar furnace was constructed at Arizona State College Tempe to investigate the material properties exposed to high heat flux [Kevane *et al.* 1957]. A solar furnace was used to generate 3500°C to measure the material properties such as thermal conductivity, thermal expansion, heat content and emissivity of different metals such Aluminum, Copper, Steel 304, Tungsten carbide, etc. for such a high temperature in the controlled environment [Glaser, 1958]. A Large furnace was constructed by National center for scientific research in Odeillo, France, having solar furnace capacity to generate 1000 kW and a temperature of more than 3800°C [Trombe 1973]. A high flux solar furnace operated by the Deutsche Forschungsanstalt fur Luft- und Raumfahrt (DLR) at Cologne can produce total power of 20 kW with peak flux densities of 4 MW/m^2. DLR furnace is used to research in the field of material science, component development and solar chemistry [Nueman *et al.* 1996]. National academy of science of Ukraine created a solar furnace which produces a temperature of 3500K for the investigation of temperature action on material. The solar furnace have been used for many applications such as research of thermo-radiational characteristics of materials, investigation of rocket space technique, service-ability of heat-shielding materials, components of military and cutting, welding, brazing of materials in vacuum [Triflov *et al.* 1999]. The solar furnace at PROMES-CNRS Odeillo is used to perform experiments to see kinetic aspects of reaction between Tantalum and Carbon under solar radiation heating. The furnace used is Medium Size Solar Furnace whose effective power is 1.5 kW and has peak density of 15M W/m^2 which can reach up to 3100 K [Fernandes *et al.* 2006]. A 40 kW solar furnace SF40 is designed and built at Platforma Solar de Almeria for the heat treatment of materials such as sintering, quenching, nitriding, carburization, foaming in controlled atmosphere. The solar furnace can focus the radiation in both horizontal and vertical plane with peak flux of 7000 kW/m^2 [Rodriguez et al. 2016]. Kováčik et al. performed experiment in solar furnace SF5 situated at Plataforma Solar de Almeria (PSA), Spain. During the experiment the Titanium powder was sintered without application of pressure

under argon atmosphere at different temperatures. Further, they compared the results obtained from solar furnace with the results obtained from vacuum furnace. They found that the porosity values dependency on temperature is almost similar for vacuum and solar furnace [Kováčik *et al.* 2017]. Chicos et al. analyzed the Microstructure and microhardness of heat treated selective laser melting manufactured Ti6Al4V alloy and published the result of heat treatment. They showed that the use of Concentrate Solar Energy in heat treatment of SLM Ti6Al4V is a suitable alternative to the conventional heat treatment. Heat treatment is carried out in SF5 and SF40 of Plataforma Solar de Almeria, Spain [Chicos *et al.* 2018]. Milosan *et al.* (2019) performed hyper-hardening heat treatment of EN 1.4136 stainless steel for its characterization by means of concentrated solar energy in one of the solar furnaces of PROMES-CNRS laboratory, in Font Romeu Odeillo (France). They concluded that the hardness values of specimen increased by 55% and the average wear rates decreased compared to the base material [Milosan *et al.* 2018]. Stoicanescu et al. discussed the use of solar energy for heat treatment of steel. They carried heat treatment of steel 1.1730 in a 5kW solar furnace SF5 of Plataforma Solar de Almeria, Spain which can reach concentration up to 600 suns and can attain temperature of 3600 K. They proved that the use of solar energy is clean and efficient in application of thermic treatment at a high industrial level [Stoicanescu *et al.* 2019]. Sonawane et al. reviewed different solar furnaces and discussed about the use of solar furnace for hardening, coatings, sintering, nitriding, synthesis, and welding of metallic materials. They concluded that it is a strong alternative of conventional method for metal processing and, it is non- contaminating, eco-friendly, economical way which can provide good quality of modified surface [Sonawane *et al.* 2020].

Generally, there are two types of furnaces based on concentrated solar thermal technologies exists, viz. directly and indirectly irradiated solar furnace. Diver *et al.* 1987 explained direct and indirect type of receiver/reactor of solar furnace. In the direct absorption receivers the sunlight directly focused to the specimen, whereas in indirect receivers an intermediate fluid is utilized to transfer heat from receiver to specimen. They also discussed the advantages, limitations and risks associated with each type of receiver/reactor. Problem associated with directly radiated solar furnace is non-homogeneous heat flux distribution which results in non-uniformity of temperature over the sample [Plaza *et al.* 2015]. Metal treatment requires homogeneity of flux over the surface to meet the desired properties; Pereira et al. performed experiment in solar furnace SF60 of Plataforma Solar de Almeria, Spain and tried to achieve homogeneous concentrated solar radiation by using homogenizers. They also compared the experimental data with the simulated data. They found that, still they cannot achieve homogeneous flux distribution over the surface, as it decreases rapidly from the centre [Pereira *et al.* 2020].

Recently a concept called solar convective furnace (SCF) is developed for heat treatment of metal [Patidar *et al.* (2015a and 2015b)]. Patidar *et al.* (2015a) argued that a SCF would be more appropriate for the heat treatment operations than a solar absorption furnace, which uses directly concentrated solar radiation to generate the process heat. The SCF based on open volumetric air receiver (OVAR) is capable of heat treatment of metals [Sharma *et al.* 2015]. In this system hot air from OVAR is transported directly or through thermal energy storage (TES) to SCF for metal treatment via forced convection. The details of SCF is presented subsequently. In this chapter a detailed investigation on solar convective furnace is presented.

4.2. SOLAR CONVECTIVE FURNACE

Solar convective furnace (SCF) is a device developed for heat treatment of metal such as annealing, soaking, tempering, etc. by convective heat transfer process. The SCF uses solar energy as a heat source instead of conventional source like electricity. The solar energy used in SCF is harnessed by using Concentrated Solar Thermal (CST) techniques. In this technology the direct

normal radiation from sun is concentrated into small area called receiver by using curved mirrors i.e. heliostat, linear Fresnel reflectors, parabolic trough or paraboloid dish [Fuqiang *et al.* 2017]. The OVAR based solar convective furnace system (SCFS) consists of, a) an OVAR on the top of central tower surrounded by a heliostat field, b) thermal energy storage (TES) and c) SCF see Figure 4. 1.

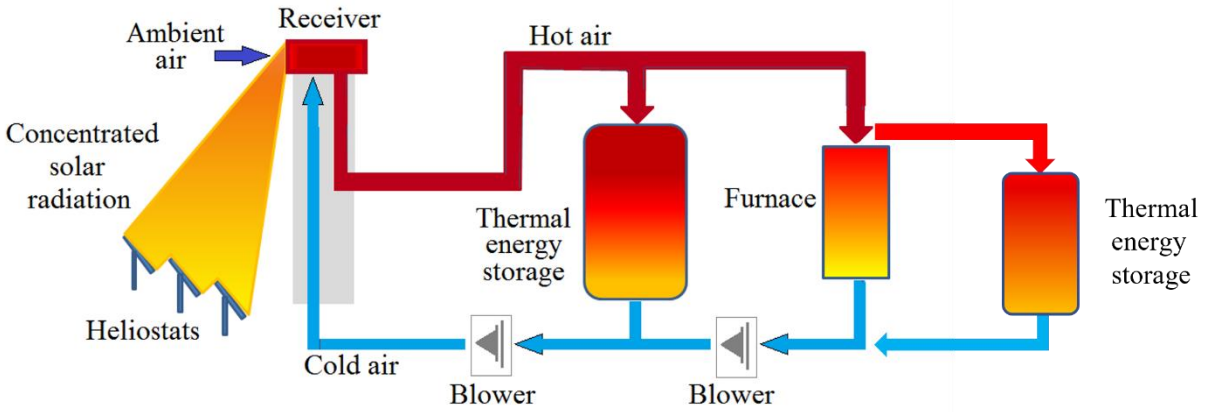

Figure 4. 1: Schematic of the solar convective furnace system

A heat transfer fluid e.g. air is used to recover heat from receiver and transported to SCF directly or through TES. The hot air transfers heat via forced convection to the metal placed inside the furnace for its treatment. The relatively cold air is then recirculated to the receiver with the help of air blower. In this system the TES stores thermal energy at daytime and supplies heat during off hours to ensure the working of system for 24 hours.

To understand the working and physics inside the convective furnace an industrial scale convective furnace is considered and described subsequently.

4.3. FULL-SCALE INDUSTRIAL FURNACE

To illustrate the concept, a full-scale industrial furnace situated in Aditya Birla Science and Technology Center; Mumbai is considered. The furnace is used for the soaking of Aluminum called Aluminum soaking furnace (ASF). The ASF can hold ten 3.2 m x 1.1 m x 0.48 m slabs, with a specific energy consumption of 400 kWh/t aluminum, and a power rating of about 0.5 MW Patidar *et al.* 2015. The schematic of full-scale industrial furnace with two Al ingots is shown in Figure 4. 2.

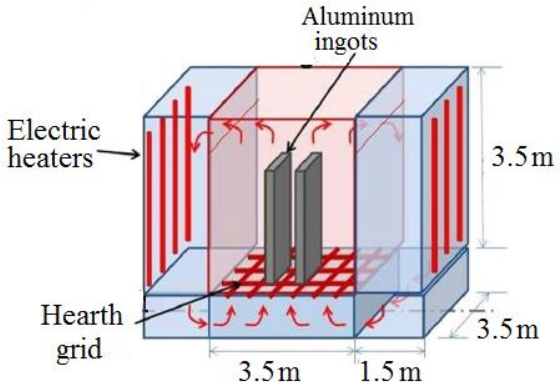

Figure 4. 2: Schematic of full-scale industrial furnace

The furnace is made up of three chambers. The central chamber called hearth of 3.5 m X 3.5 m X 3.5 m is for heat treatment. The two side chambers are of 3.5 m X 3.5 m X 1.5 m mounted with electric heaters which is used for heating of air. The heated air is circulated in the furnace using blower. The hot air enters the central chamber through the bottom called hearth grid and transfers heat to placed ingots via forced convection. The relatively cold air leaves the chamber from top and re-circulated to side chambers. In ASF, Al-ingots are heated from 100 to 600 °C in six hours and kept at 600 °C for four hours. The dimensions and the operating conditions of the industry scale furnace are given in Table 4. 1.

Table 4. 1: Dimensions and operating conditions of a full-scale Industrial furnace

Parameters	**Values**
Hearth dimension (m × m × m)	3.5 x 3.5 x 3.5
Ingot dimension (m × m × m)	3.2 x 1.1 x 0.48
Spacing between ingots (m)	0.24
Inlet air temperature (^{0}C)	650
Ingot initial temperature (^{0}C)	100
Ingot final temperature (^{0}C)	600
Time taken for heating (hr)	10.5
Biot number	0.03
Fourier number	57.4
Surface-area averaged heat transfer coefficient (W/m^{2}K)	26

4.4. RETROFITTED SCALE-DOWN SOLAR CONVECTIVE FURNACE

The existing industrial convective furnace is retrofitted to use solar energy instead of conventional electric power for heating. The retrofitted solar convective furnace is shown in Figure 4. 3. The hot air from receiver or TES will be introduced from the top of the side chambers which further enter to central chamber/hearth from bottom for the heat treatment of metal. The air flow path is shown by arrows in Figure 4. 3.

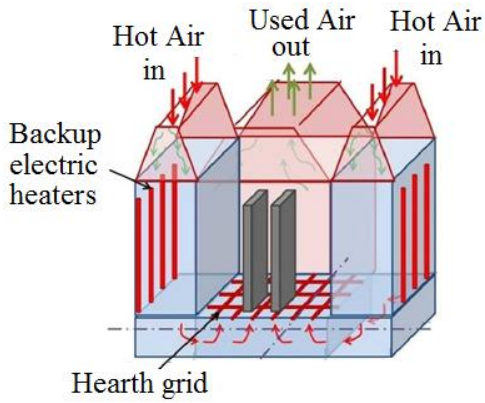

Figure 4. 3: Schematic of retrofitted Solar convective furnace.

For investigation the industrial furnace is scaled down in the ratio of 1:15 by ensuring geometrical and kinematic similarity [Patidar *et al.* (2015a and b)]. The detailed scaling is explained in following sub-section.

4.5. PART-SCALE DOWN MODEL

The ingots arrangement inside the furnace is shown in Figure 4. 4, all are placed symmetrically. The heat transfer in each ingot will be same as the air flow will is distributed equally. So, evaluation of one ingot will be sufficient to understand the process. Hence, a part scale-down SCF model is fabricated to perform experiments, which treats a single metal-ingot at a time as shown with dotted lines in Figure 4. 4.

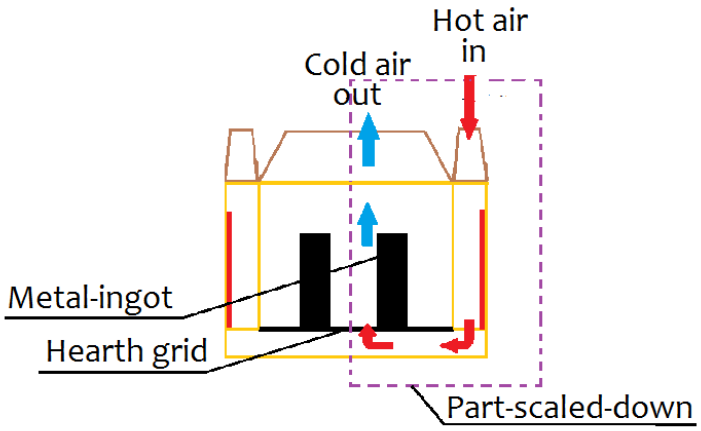

Figure 4. 4: Schematic of part of scale-down model

A schematic diagram of the retrofitted laboratory furnace system is shown in Figure 4. 5. It consists of a furnace that is attached to an external heater unit (EHU). The furnace is externally insulated using 25 mm thick glass wool, which is covered with a 0.5 mm thick aluminum sheet. The furnace consists of two sections, namely the hearth and the heating section; its dimensions are shown in Table 1. A steel sheet (200 mm x 200 mm x 16 mm thick) is placed on steel support containing six 20 mm diameter holes. The thickness of the steel sheet ensures that the Biot number (Bi) is less than 0.1 as in an industrial ASF Patidar 2015. Hot air from TES flows downwards into the heating section

and upwards through the hearth where it transfers heat to the steel sheet. The holes in the steel support facilitate the uniform distribution of air in the hearth. The gaps adjacent to the top of the metal sheet are referred to as the hearth outlet. To prevent the heat transfer from the hearth to the heating section, 25 mm glass wool insulation was placed on both sides of the separating wall.

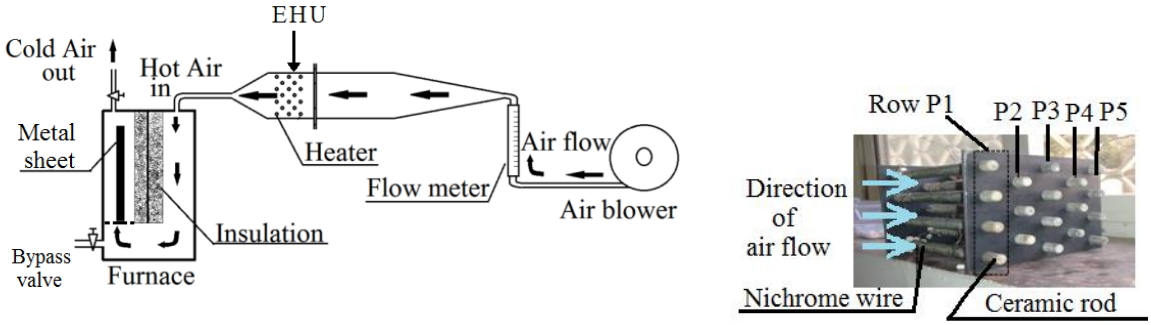

Figure 4. 5: 2D schematic of the solar convective furnace with an external heater unit (EHU)

The dimensions of the experimental furnace and metal slap are summarized in Table 4. 2.

Table 4. 2: Dimension of experimental furnace and steel sheet

Parameters	**Values**
Hearth dimension (height × width × depth) (m)	0.235 × 0.031 × 0.235
Steel sheet dimension (height × thickness × width) (m)	0.2 × 0.016 × 0.2
Gap between slab and furnace walls (mm)	7.5

To compensate for any energy shortage, the retrofitted furnace retains the electrical heater in the heating section and is also provided with an EHU. The EHU consists of eighteen 100 mm long and 7 mm diameter alumina rods, which are arranged in a staggered manner (Figure 4. 6). This is characterized by rod diameter (D), transverse (St), and longitudinal (Sl) pitches, see Figure 4. 6.



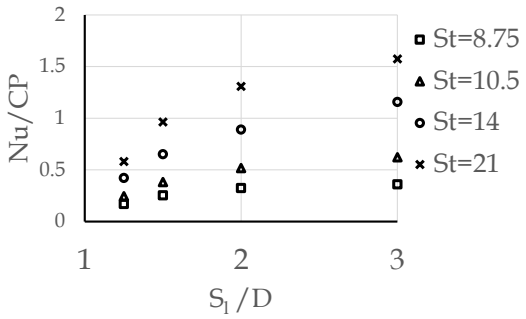

(c)

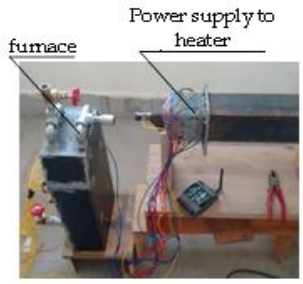

(d)

Figure 4. 6: (a) A schematic illustrating cross flow around the ceramic rods of electrical heater in EHU, (b) staggered arrangement of alumina rods with relevant geometrical parameters, (c) calculated FoM for different staggered arrangements of ceramic rods and (d) installed power supply to the heating elements

The cross-flow of air is chosen for the inherent heat transfer advantages (Figure 4. 6a). Now, a figure-of-merit (FoM) is defined as the ratio of Nusselt number (Nu) to coefficient-of-pressure (CP). A high value of FoM is desired for obvious reasons. This parameter is estimated using the available correlations and expressions, in Eq. (4.1) – (4.4), see e.g. Incropera (2007), Hammock (2011).

$$Nu = C.Re_{D,max}^{m}.Pr^{0.36}.\left(\frac{Pr}{Pr_s}\right)^{1/4} \tag{4.1}$$

$$\Delta P = \frac{2fG_{max}^2 N_L}{\rho}\left(\frac{\mu_s}{\mu}\right)^{0.14} \tag{4.2}$$

$$f = \left(0.25 + \frac{0.118}{(\frac{St-D}{D})^{1.08}}\right).Re_{max}^{-0.16} \tag{4.3}$$

$$CP = \frac{\Delta P}{\frac{1}{2}\rho {v_\infty}^2} \tag{4.4}$$

For the heater, Sl/D = 1.25, 1.50, 2.00, and 3.00 with St = 8.75 mm, 10.75 mm, 14.00 mm, and 21.00 mm are used, benefitting from the findings of Khan (2006). The ceramic rods are arranged in five rows (N_L =5) following Incropera (2007). Calculations for FoM show that St=21.00 mm and Sl/D = 3 may be preferred for EHU (Figure 4. 6c). The ceramic rods are wrapped with a 1 m long Nichrome wire having a diameter of 0.4 m for electrical heating (Figure 4. 6d). The rod material has resistivity ~ 10^{14} Ω-cm and withstands a temperature up to 1000°C. Nine K-type thermocouples, T1 to T9, are mounded on the steel sheet (metal sheet) to record its surface temperature, and ten thermocouples (denoted by T_{i1}, T_{o1}, etc.) are mounted at the inlet and outlet to SCF for recording the air temperature before and after the metal sheet, respectively (see Figure 4. 7). These thermocouples are calibrated with Isotech PEGASUS RS 422. An uncertainty of 1-2% for measuring up to 300 ºC is noted.

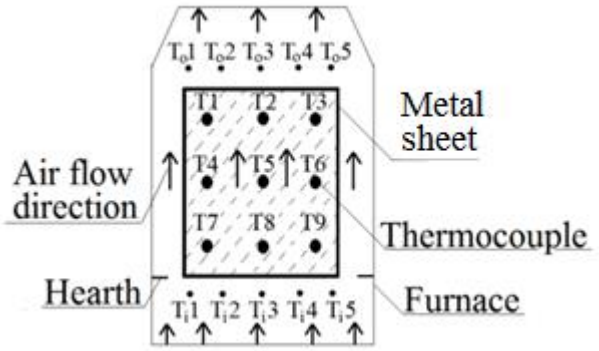

Figure 4. 7: The installed k-type thermocouples for temperature measurement of air and metal sheet

4.6. METHODOLOGY

Whole experiment is performed in two stages viz. i) preheating and ii) metal processing. In preheating phase, the air bypassed through bypass valve to preheat the furnace internals. After achieving pre-defined temperature, the air is directed towards metal ingot for metal processing.

4.6.1. SCF with heater

A preliminary experiment with main heater is performed in SCF. The schematic of part-scale down furnace including main heater with air flow path is shown in Figure 4. 8. Figure illustrates hot air generated in heater is introduced in the furnace through the inlet duct. In first phase hot air is by-passed to ambient through a by-pass valve mounted at the bottom of hearth to preheat the furnace internals during the first phase (see Figure 4. 8a). This is necessary to obtain a high temperature air at the inlet to hearth. In the second phase i.e. metal processing phase hot air flows around the metal-ingot inside the hearth. The resulting heat transfer to metal-ingot via forced convection is inferred by its temperature rise. The relatively cold air at the furnace outlet is released to atmosphere or stored (see Figure 4. 8b). This is termed as SCF operation with a heater. The experimental conditions for SCF operation with a heater are summarized in Table 4. 3.

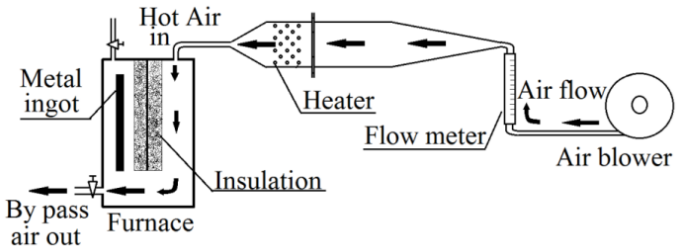

a)

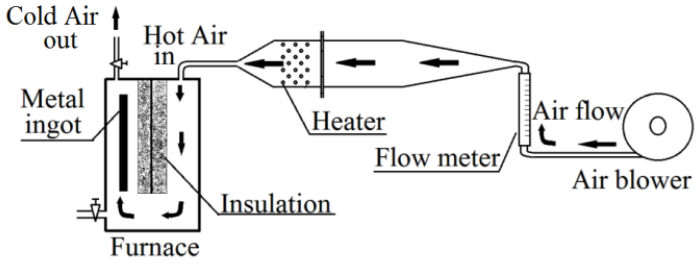

Figure 4. 8: A schematic showing the (a) furnace preheating, and (b) metal processing phase

Table 4. 3: The experimental conditions for SCF operation with a heater

Parameter	Values
Power supplied to heater (kW)	0.7 (± 5%)
Mass-flow-rate (kg/s)	0.007 (± 5%)
Air by-pass time (s)	2500
Metal processing time (s)	5300

4.6.2. SCF with TES

The same process is adapted in this case, the only difference is the hot air is coming from charged TES instead of heater. The air flow path is shown in Figure 4. 9, and depicted by red in color traveling from outlet of TES1 (point 'B') to inlet of SCF at point C. The hot air passes through inlet duct of SCF and bypassed through the by-pass valve at the bottom of hearth in preheating phase. In metal processing phase the hot air is directed towards the metal ingot. The process is continued until the target is reached. The heater may be used when the available energy at TES1 lowers the required energy at SCF inlet. The data of experiment 1 is selected and presented in subsequent section for the analysis.

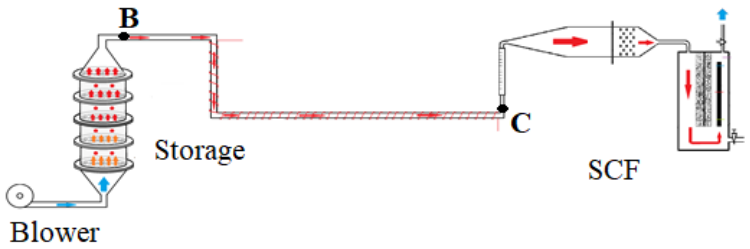

Figure 4. 9: Schematic of air flow path for metal processing in SCF using TES1.

4.7. EXPERIMENTAL RESULTS

4.7.1. SCF with heater

As explained in previous sub-section the experiment is performed in two stages which are discussed in this sub-section. Temperature values of air and metal ingot are measured at different location which are explained as follows.

Stage I (Preheating): In this stage, ambient air is heated in main heater and bypassed to atmosphere. The air flow path of this stage is shown Figure 4. 8a. The air is circulated with the help of air blower mounted in the system. During preheating stage, the *bypass valve* is opened, and *outlet valve* is closed for 2500 seconds. In this stage, air is not allowed to go towards the metal-ingot, however natural convection is expected to setup in the gap between furnace wall and metal-ingot which results increment in temperature of metal ingot. The following are observed through the measurements:

a) The temperature of air at inlet increases from 33 °C to 82 °C (see Figure 4. 10). During this process wall of inlet duct is pre-heated by hot air via forced convection. The temperature of air at outlet also increases from 33 °C to 60 °C (see Figure 4. 10). this is due to natural convection occurring in gap.
b) The temperature of metal-ingot at points T2, T5 and T8 increases from 33 °C to ~50 °C. The rate of temperature rise is ~0.4°C/minute. It is seen that the steel-ingot at the hearth inlet i.e. point T2 is at higher temperature than that of furnace outlet i.e. at point T8. Which is indeed since the heat transfer rate the inlet is higher than that of outlet. The temperature values are shown in Figure 4. 10.

Stage II (Metal processing): After preheating the bypass valve is closed and hot air is directed towards metal ingot from the bottom of the hearth grid. Simultaneously the outlet valve is opened. Consequence the hot air starts transferring heat to metal-ingot via forced convection, the relatively cold air them released to ambient through outlet valve. The air flow path of metal processing stage is shown Figure 4. 8b. Metal processing is done for next 5300 seconds. The following observations are made during this stage:

a) The temperature of air at inlet increases rapidly from 82 °C to 95 °C within 100 seconds. Further it increased gradually to reach target maximum temperature of 130 °C in next 5200 seconds (see Figure 4. 10a). Similarly, the temperature of air at outlet increases from 60 °C to 120°C at the end of 7800 seconds. Interestingly, same as at inlet, a sharp rise from 60 °C to 70°C within 100 seconds is seen at outlet position, this shows the transition process from stage 1 to 2. So, a proper operational time which accounts transition time is necessary. Thus, manual operation should be avoided by including electronic controlled valves.
b) The temperature rise in metal-ingot follows similar trend to that of inlet and outlet temperature of as shown in Figure 4. 10a. The temperature of metal ingot remained lower than of air temperature throughout the time, however at the end of experiment the outlet temperature of air and temperature at T8 and T5 becomes almost equal to reach towards steady state. The temperature values of points T2, T5 and T8 with respect to time is shown in Figure 4. 10a. A maximum temperature difference of about 20°C on the steel-ingot along the height is seen at early phase of preheating stage, which reveals that at initial stage the rate heat transfer from hot air to metal ingot is more at lower part of ingot. As time elapsed, the temperature difference along the height starts decreasing due to thermal diffusion within the metal-ingot. So, it is necessary to keep the length of metal-ingot optimum, for least temperature difference along the height to avoid generation thermal stress within the metal-ingot.
c) The metal-ingot temperature at the mid-plane shown by T4, T5 and T6 are practically same (see Figure 4. 10b) which confirms the thermal uniformity along the thickness of metal-ingot. This ensured the selection of $Bi \sim 0.03$

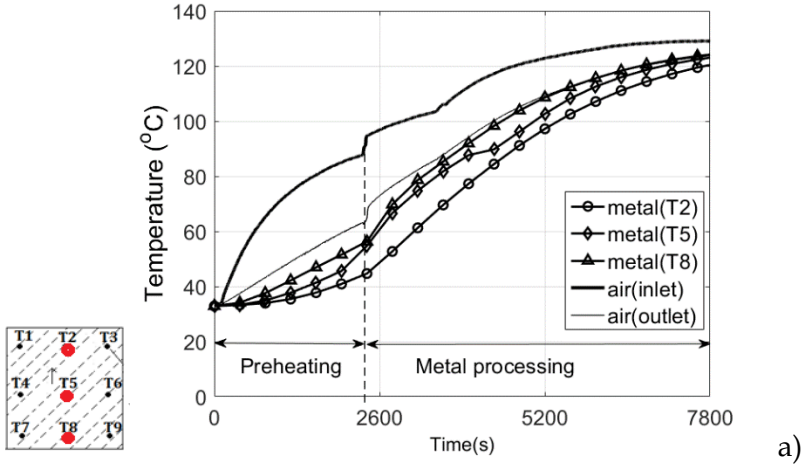

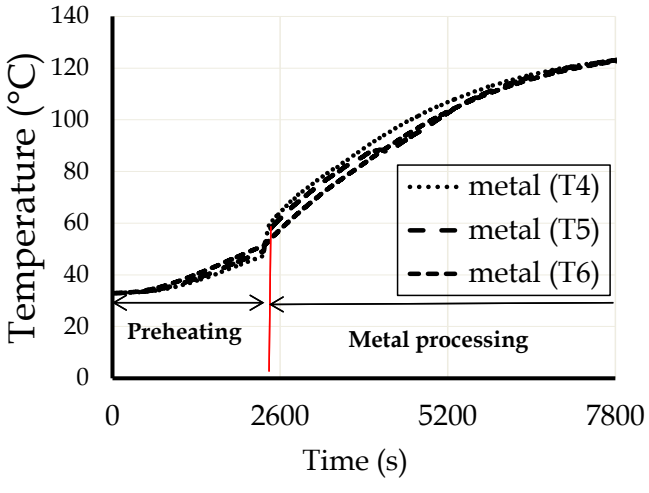

Figure 4. 10: The measured temperature of a) air and metal ingot temperatures at different positions inside the furnace b) temperature at mid-section of metal-ingot

4.7.2. SCF with TES

Figure 4. 11 depicts the measured air and metal temperature at the SCF and hearth inlets, three locations along with height (TC2, TC5, TC8), and the SCF and hearth outlets. The hot air from TES1 is transported through the relatively cold 6 m long pipeline to the SCF (see Figure 4. 9). Thus, a significant drop in the air temperature at the SCF inlet is expected. Figure 4. 11 shows that the temperature of the metal sheet is highest near the hearth inlet (TC8) and lowest near the hearth outlet (TC2). At higher air temperatures, this difference would have been more significant in the initial phase of metal processing. Also, the differences gradually reduce with the processing time, which depicts the heating and internal redistribution of heat in the metal ingot. Because of the heat transfer to the long cold pipeline, heat treatment occurred at low temperatures. This can be mitigated just by preheating the piping network. Figure 4. 12 shows that the temperature is uniform across the width of the metal sheet.

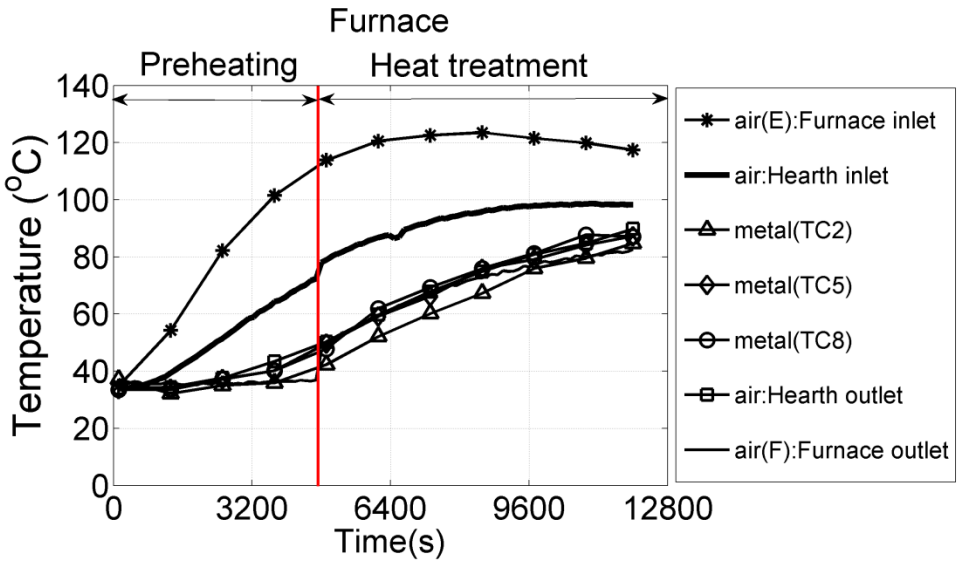

Figure 4. 11: The measured metal slab surface temperature along the height in SCF for experiment 1

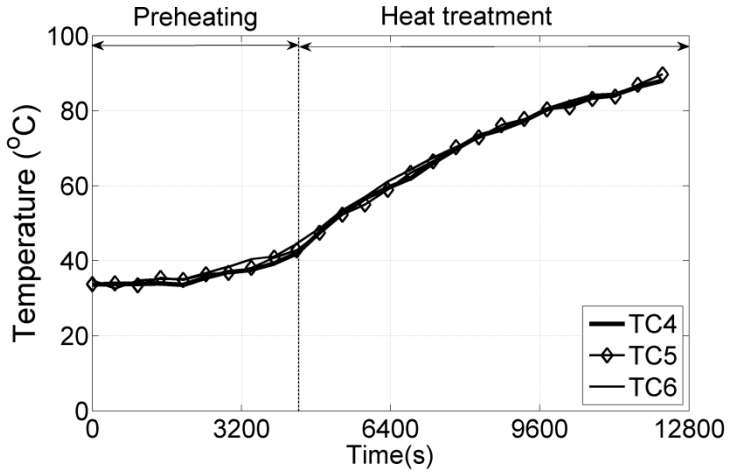

Figure 4. 12: The measured metal sheet surface temperature, along the width, at centreline, for experiment 1

4.8. SUMMARY & CONCLUSIONS

This chapter presents experiment-based assessment of the retrofitted solar convective furnace (SCF). The SCF is 1:15 scale down model of an industrial furnace. The experiments are performed for heating of a carefully-selected steel ingot, satisfying Bi < 0.1 as in the industry scale furnace, via forced convection. The experiment is performed in two phases viz. SCF preheating and metal processing/heat treatment in SCF. The SCF is preheated for 2600 seconds using an installed backup electrical heater or by using the bypass of hot air. During this process the average metal ingot temperature increases from 33°C to 60°C by natural convection. Afterwards, metal processing is initiated by forced convection of hot air around the metal ingot for about 5200 seconds. During this process the metal ingot temperature rises up to 130 °C. The experiment clearly reveals that thermal uniformity of metal ingot, along the height, increases with the time. Also, the operation reveals stable condition, which is desired for the heat treatment process. As a logical next step the assessment of integrated SCF system is reported.